Junctional Adhesion Molecule, a Novel Member of the Immunoglobulin Superfamily That Distributes at Intercellular Junctions and Modulates Monocyte Transmigration

Inés Martìn-Padura,* Susan Lostaglio,* Markus Schneemann,‡ Lisa Williams,‡ Maria Romano,* Paolo Fruscella,* Carla Panzeri,§ Antonella Stoppacciaro,‖ Luigi Ruco,‖ Antonello Villa,§ David Simmons,‡ and Elisabetta Dejana*

*Istituto di Ricerche Farmacologiche Mario Negri, 20157 Milano, Italy; ‡Institute of Molecular Medicine, University of Oxford, John Radcliffe Hospital, Headington, Oxford, OX3 9DU, United Kingdom; §Dipartimento di Farmacologia, Universita degli Studi di Milano, and DIBIT, Milano, Italy 20129; and ‖Universita' degli Studi La Sapienza, Dipartimento di Medicina Sperimentale e Patologia, 00161 Roma, Italy

Abstract. Tight junctions are the most apical components of endothelial and epithelial intercellular cleft. In the endothelium these structures play an important role in the control of paracellular permeability to circulating cells and solutes. The only known integral membrane protein localized at sites of membrane–membrane interaction of tight junctions is occludin, which is linked inside the cells to a complex network of cytoskeletal and signaling proteins. We report here the identification of a novel protein (junctional adhesion molecule [JAM]) that is selectively concentrated at intercellular junctions of endothelial and epithelial cells of different origins. Confocal and immunoelectron microscopy shows that JAM codistributes with tight junction components at the apical region of the intercellular cleft. A cDNA clone encoding JAM defines a novel immunoglobulin gene superfamily member that consists of two V-type Ig domains. An mAb directed to JAM (BV11) was found to inhibit spontaneous and chemokine-induced monocyte transmigration through an endothelial cell monolayer in vitro. Systemic treatment of mice with BV11 mAb blocked monocyte infiltration upon chemokine administration in subcutaneous air pouches. Thus, JAM is a new component of endothelial and epithelial junctions that play a role in regulating monocyte transmigration.

Key words: endothelium • epithelium • monocyte • tight junctions • inflammation

I᙮ is currently believed that leukocytes leave the circulation by first adhering to endothelial cells and then migrating through the interendothelial junctions (32, 50). This last process implies the transient opening of interendothelial contacts allowing leukocytes to transmigrate through the adjacent endothelial cells (16).

At least two types of cell to cell junctional structures have been identified in the endothelium: adherens junctions (AJ)[1] and tight junctions (TJ; 16, 45). These organelles present common features in endothelial (EC) and epithelial cells. AJ are formed by clusters of transmembrane proteins belonging to the cadherin family linked intracellularly to catenins (β-catenin, plakoglobin, p120), which in turn promote anchoring to the actin cytoskeleton (15, 26, 28, 31, 33, 35, 52).

The molecular organization of TJ is less understood. The first transmembrane protein identified is occludin (21), which is directly bound intracellularly to zonula occludens-1 (ZO-1), a member of the MAGUK family (membrane-associated guanylate kinases; 22). A number of other cytoplasmic proteins have been reported to be associated with the plaque structure underlying TJ, such as ZO-2, 130-kD protein, 7H6 antigen, cingulin, symplekin (34), and others (for review see references 3, 4, and 11).

How leukocytes traverse intercellular junctions and disrupt their fine organization is still largely unknown. It was found that PECAM-1 (platelet endothelial cell adhesion molecule-1, CD31), a member of the immunoglobulin gene superfamily (IgSF) located at interendothelial junc-

tions, is required for leukocyte transmigration (7, 38, 55, 60). PECAM-1 is not associated with either AJ or TJ structures (5).

To characterize further the molecular organization of intercellular junctions in the endothelium and to define their role in leukocyte transmigration, monoclonal antibodies directed to mouse EC (56, 24) were used to screen for antigens located at cell–cell contacts. A mAb, BV11, was found to label endothelial and epithelial intercellular junctions selectively in a region close to TJ. Expression cloning revealed that BV11 recognizes a new member of the IgSF (8, 29). Monocyte transmigration was inhibited by mAb BV11 both in chemotaxis assays in vitro and in a model of skin inflammatory reaction in vivo.

Materials and Methods

Cells

Mouse EC, 1G11, kindly provided by A.Vecchi (Mario Negri Institute, Milan, Italy), were obtained from mouse lung microcirculation, maintained in DMEM (GIBCO BRL, Paisley, Scotland), supplemented with 10% FCS, 50 μg/ml endothelial cell growth supplement (prepared from bovine brain), and 100 μg/ml heparin (Sigma Chemical Co, St. Louis, MO), and used within passage 15 (17). H5V, a mouse EC line derived from primary cultures of mouse heart endothelial cells immortalized by polyoma virus middle T antigen, were also provided by A.Vecchi and characterized in detail elsewhere (25). Mouse epithelial cells (PDV), kindly provided by A. Cano (Instituto de Investigaciones Biomedicas, Madrid, Spain), were skin keratinocytes isolated and cultured as previously described (23). Monocytes were obtained from the peripheral blood of normal healthy donors as reported in detail (14). CHO cells and SP2/0 were obtained from American Type Culture Collection (Rockville, MD). CHO cells were transfected by calcium phosphate precipitation method with 20 μg of pECE-junctional adhesion molecule (JAM) and 2 μg of pB-SpacDp plasmids as previously described (10). Then, cells were cultured in selective medium with puromycin (Sigma Chemical Co.), and the resulting resistant colonies were isolated and tested for BV11 antigen (JAM) expression by immunofluorescence staining and immunoprecipitation analysis. Positive cells were cloned and expanded for further studies as described (10).

Vascular endothelial (VE)-cadherin and N-cadherin transfectants were produced and cultured as reported (40). VE-cadherin truncated mutant was produced and characterized previously (39). This mutant lacks the intracellular domain responsible for binding to catenins and to the actin cytoskeleton.

Antibodies

mAbs BV11 and BV12 were generated in our laboratory following a previously described procedure (56). In brief, male Lewis rats were immunized with H5V endothelial cells with successive intraperitoneal injections. 3 d after the final boost, rat spleen cells were fused with the SP2/0 mouse myeloma cells and grown in selective medium. Culture supernatants of hybrid clones were screened for reactivity on H5V cells by an ELISA test (56) and in immunofluorescence microscopy for their ability to decorate intercellular contacts (36).

In further studies, the two mAbs were found to be positive in ELISA for binding to a recombinant JAM (BV11 antigen, see below) Fc fusion protein consisting of the NH$_2$-terminal domain of the protein up to amino acid 132, prepared and purified as described previously (19, 20). However, by cross-competitive mAb-binding assay performed as described elsewhere (37), BV12 was unable to inhibit radiolabeled BV11 binding. This result strongly suggests that the two mAbs recognize a different epitope. F(ab′) fragments of BV11 were prepared by standard procedures (41).

mAb MEC 14 to CD34 was kindly provided by A. Vecchi (24). Hybridoma-producing mAb MK 2.7 and mAb HB151 of the same isotype (IgG2b) of BV11 were obtained from American Type Culture Collection and used as controls.

The antibodies used in fluorescence microscopy were as follows: rat mAb anti-E-cadherin DECMA (Sigma Chemical Co); rat mAb anti-ZO-1, R40.76 kindly provided by B. Stevenson (University of Alberta, Canada; reference 51); rabbit polyclonal antibody to cingulin by S. Citi (Università di Padova, Padova, Italy; references 12 and 13); rabbit polyclonal antibody to VE-cadherin by D. Vestweber (Institute of Cell Biology, Münster, Germany; reference 9); and rabbit polyclonal antibody to β-catenin (Transduction Laboratories, Lexington, KY) and to occludin (Zymed Laboratories, Inc., San Francisco, CA). As secondary antibodies, FICT-conjugated Affinipure donkey anti–mouse, anti–rabbit, and TRICT-conjugated anti–rat IgG with minimal cross-reaction with other species (Jackson ImmunoResearch Laboratories, Inc., West Grove, PA) were used.

Fluorescence Flow Cytometric Analysis

Fluorescence flow cytometric analysis was performed by a FACStar Plus™ apparatus (Becton Dickinson, Mountain View, CA) using an FICT-conjugated goat anti–rat antiserum (mouse adsorbed; Caltag Laboratories, Burlingame, CA) as described in detail elsewhere (37).

Immunofluorescence Microscopy

Immunofluorescence analysis of antibody staining of the cells was as described (36). In brief, cells were seeded on glass coverslips and grown to confluence. Cells were then fixed with methanol for 3 min at −20°C and processed for indirect immunofluorescence microscopy.

For occludin staining, fixation was followed by subsequent incubation with PBS-0,1% saponin (Sigma Chemical Co.) for 10 min, and with 0.1% PBS, 0.5% saponin BSA for 10 min.

Coverslips were then mounted in Mowiol 4-88 and examined with an immunofluorescence microscope (Axiophot; Carl Zeiss, Oberkochen, Germany), and images were recorded on T MAX P3200 films (Eastman Kodak Co., Rochester, NY).

Double-staining immunofluorescence was analyzed by confocal microscopy as described (42). Confocal microscopy was carried out on an MRC 1024 microscope (Bio-Rad Laboratories, Hercules, CA) equipped with a krypton/argon laser. Noise reduction was achieved by Kalman filtering during acquisition. The images were then recorded using a Focus Imagerecorder Plus image recorder (Focus Grafics, Inc., Grafite, Vimercate, Italy) and printed with a Seiko FII ColorPoint 2 (Grafite).

Immunohistochemistry

Organ specimens of adult and newborn mice and 14-d fetuses were obtained and snap-frozen in isopentane cooled by liquid nitrogen to about −140°C as reported (24, 42). Frozen tissues were sectioned (7 μm) with a CM 10800 cryostat (Leica Inc., Deerfield, IL), mounted on gelatine-treated coverslips, briefly air-dried, and then fixed in −20°C acetone for 10 min. After fixation, samples were washed twice with PBS and quenched with 0.1 M glycine for 5 min.

For immunofluorescence confocal microscopy, primary antibodies were incubated for 30 min followed by three 5-min washes with PBS before applying secondary antibodies for 30 min. After antibody binding, samples were washed and then mounted. Confocal microscopy was carried out as mentioned above (42).

For immunohistochemistry, sections were incubated with mAb BV11 after quenching, and immunostained using a biotinylated affinity-purified anti-rat Ig (Sigma Chemical Co.) and streptavidin–HRP complexes (Sigma Chemical Co). Samples were then counterstained with hematoxylin, mounted, and analyzed as previously reported (24).

Immunoelectron microscopy was performed as previously described in detail (57). A rabbit antiserum raised by injecting a JAM recombinant fragment consisting of the NH$_2$ domain up to amino acid 132 under the form of Fc fusion protein (19, 20) was used. Immunization procedures were as described (20). The JAM recombinant fragments were produced and purified as described previously (19, 20). The preimmune serum and serum from immunized rabbits were tested in ELISA, immunofluorescence, and immunoprecipitation of JAM-CHO transfectants and cultured endothelial cells (H5V; see below).

For immunogold labeling, ultrathin cryosections (50–100 nm–thick) were collected over nickel grids and covered with 2% gelatin. After treatment with 125 nM Na phosphate buffer (pH 7.4) supplemented with 0.1 M glycine, the cryosections were exposed for 1 h at 37°C to the first antibody diluted in phosphate–glycine buffer, and were then washed with the buffer and decorated with anti IgG-coated gold particles (6 nm) exactly as described elsewhere (57).

cDNA Expression Library and Cloning

cDNA expression library was constructed from a murine brain EC line (bEnd.3; 19, 46, 47, 49). The cDNA library was oligo-dT primed bEnd.3 polyA$^+$ RNA cloned into pCDM8. Three rounds of expression and panning yielded a single clone insert of ∼2 kb. The pCDM8 inserts were rescued and subcloned in pBluescript vector and sequenced. The nucleotide and deduced protein sequences were screened against the GenBank/EMBL database using a FASTA/BLAST programs as implement on the Internet resource.

Northern Blot

A multiple tissue Northern blot of mouse tissues (CLONTECH Laboratories, Inc., Palo Alto, CA) containing ∼2 μg of polyA$^+$ RNA per lane was hybridized with a 1.3 XbaI fragment from the JAM cDNA clone, labeled with [^{32}P]dCTP by random priming as described (49). Hybridization was performed at 65°C in ExpressHyb hybridization solution (CLONTECH Laboratories, Inc.), washed according to the manufacturer's protocols, and autoradiographed on Kodak X-Omat AR film at −70°C (49).

Immunoprecipitation and Immunoblot

Biotinylation and immunoprecipitation procedures are described elsewhere (39). In brief, biotinylation of cell surface proteins was performed using sulfonitrohydroxysuccinimidobiotin (Pierce Chemical Co., Rockford, IL). Whole cell extracts were obtained from confluent cells and immunoprecipitated with protein A-Sepharose CL-4B (Pharmacia Biotech Sverige, Uppsala, Sweden) coupled with rabbit anti–rat Ig (Sigma Chemical Co). Then samples were fractionated under reducing conditions on 7.5% SDS-PAGE gels, transferred to nitrocellulose membranes, and incubated with HRP-streptavidin (Biospa Division, Milano, Italy). The HRP-streptavidin was visualized using an enhanced chemiluminescence kit (Amersham International, Buckinghamshire, United Kingdom) and autoradiography as previously described (39).

Cell Transmigration Assay

Monocyte chemotaxis through EC monolayers were performed as previously described (43). In brief, EC (IG11 and H5V) were cultured in Transwell units (with polycarbonate filter, 8-μm pore; Costar Corp., Cambridge, MA) to confluency. mAbs were added to EC monolayers for 30 min at 37°C, and were then kept throughout the transmigration assay. Most of the experiments were done using purified BV11 mAb at 5 μg/ml or hybridoma culture supernatant diluted 1:2, which are saturating concentrations by FACS analysis of both EC lines in suspension. All the other mAbs were used at a concentration of 1:2 dilution of hybridoma culture supernatant.

Washed monocytes (14) were labeled with ^{51}Cr and then resuspended at 1.8×10^6 cells/ml in complete medium. An aliquot (750 μl/well) of radiolabeled monocytes was added and incubated for 60 min at 37°C. In some experiments, the chemokines monocyte chemotactic protein-1 (MCP-1) and MCP-3 (100 ng/ml; Peprotech, EC ltd., Rocky Hill, NJ) were added in the lower chamber. In other experiments, EC monolayers were incubated with lipopolysaccharide (LPS; 50 ng/ml in complete medium, *Escherichia coli* 055:B5; Sigma Chemical Co.) for 24 h, and were then washed before monocyte addition.

At the end of the transmigration assay, nonadherent monocytes were removed from the upper chamber (nonadherent fraction). Transmigrated cells were both collected from the lower chamber medium and removed by scraping the opposite face of the filter (migrated fraction). Adherent monocytes together with the intact EC monolayer were then collected from the polycarbonate membrane (adherent fraction). Radioactivity of the three fractions was measured in a γ-counter (Beckman Instruments, Inc., Fullerton, CA), and the number of cells in each fraction was quantitated as described (43).

Permeability Assay

Permeability across cell monolayers was measured in Transwell units (with polycarbonate filter, 0.4-μm pore; Costar Corp.) as previously described (10). In brief, CHO transfectants were cultured to confluency for 5 d. Then, culture medium was replaced with serum-free medium, and FITC-dextran (1 mg/ml, average molecular mass of 38,900; Sigma Chemical Co.) was added to the upper chamber. At 2 h, 100-μl aliquots were collected from the lower compartment and assayed by fluorimetry (excitation wave-

length set at 492 nm and emission at 520 nm). In some experiments, EGTA (5 mM final concentration) was added both to lower and upper compartments for 1 h at the same time as dextran (10).

Air Pouch Model

The air pouch model procedure was described in detail elsewhere (18, 44). In brief, after a period of adaptation, male CD1 mice (20–22 g) were anesthetized with ether, and 5 ml of sterile air was injected dorsally subcutaneously (day 0). 3 d later, pouches were reinjected with 3 ml of sterile air. On day 5, animals received intravenous injection of either 100 μg or 200 μl of mAb BV11, the same dose of an irrelevant purified mAb of the same isotype (clone HB151), or 200 μl of saline. On day 6, 1 μg of MCP-3 dissolved in 1 ml of carboxymethylcellulose (0.5% in saline; Fluka AG, Buchs, Switzerland) was injected into the pouch. After 1 h, animals were killed and the pouches were washed with 1 ml of saline (see Fig. 9). The lavage fluid was immediately cooled on ice, and the volume was recorded. 50-μl aliquots were used for cell counting after staining with erythrosin as described (44).

Results

BV11 Antigen Distributes at Intercellular Junctions in Endothelial and Epithelial Cells

Fig. 1 reports the staining pattern of BV11 in cultured endothelial cells and in intact vessels in vivo. The mAb decorated cell–cell contacts in cultured EC (Fig. 1 *A*) in a way similar to other junctional markers such as ZO-1 (Fig. 1 *B*) or VE-cadherin (Fig. 1 *C*). In vivo, the mAb retained a typical staining pattern at endothelial cell–cell contacts (Fig. 1 *E*). At confocal microscopy, double-label immunofluorescence analysis of tissue cryosections shows that in vessels mAb BV11 distributed closely to TJ markers such as cingulin (Fig. 1, *D–F*) or occludin (not shown).

BV11 mAb was not specific for EC, but could recognize epithelial cells of different origins (Fig. 2, *A–F*). Higher resolution analysis by confocal microscopy of cultured epithelial cells revealed that the BV11 antigen is concentrated at the apical region of the intercellular cleft (Fig. 2, *B b*) in a way similar to TJ components such as ZO-1 or occludin (not shown). Double-label immunofluorescence analysis shows a good codistribution of the antigen with TJ-specific components such as cingulin (Fig. 2, compare *A a*, *B b*, and *C c*) or occludin (not shown). In contrast, AJ components such as β-catenin or E-cadherin gave a more diffuse staining along the intercellular cleft (34 and see below), and at confocal microscopy did not codistribute with BV11 antigen (not shown).

In tissue sections, BV11 was concentrated at the subapical domain of epithelial cell–cell contacts. A typical example is reported in Fig. 2 (*D–F*), which shows mAb BV11 staining of the epithelium of mouse duodenum. BV11 was restricted to a TJ-containing narrow apical region of the cleft (Fig. 2 *E*). In contrast, AJ marker proteins such as β-catenin (Fig. 2 *D*) or E-cadherin (not shown) displayed a more diffuse distribution all along the lateral wall of the cells. Very little if any codistribution of BV11 and β-catenin could be observed (Fig. 2 *F*).

Immunogold labeling of ultrathin sections of the epithelium of mouse duodenum revealed that BV11 antigen was concentrated in the tight junction area, while no specific staining was found in adherens junctions (*zonula adherens)* and desmosomes (Fig. 3, *A* and *B*). In some sections (see Fig. 3 *B*) the immunogold labeling was observed also
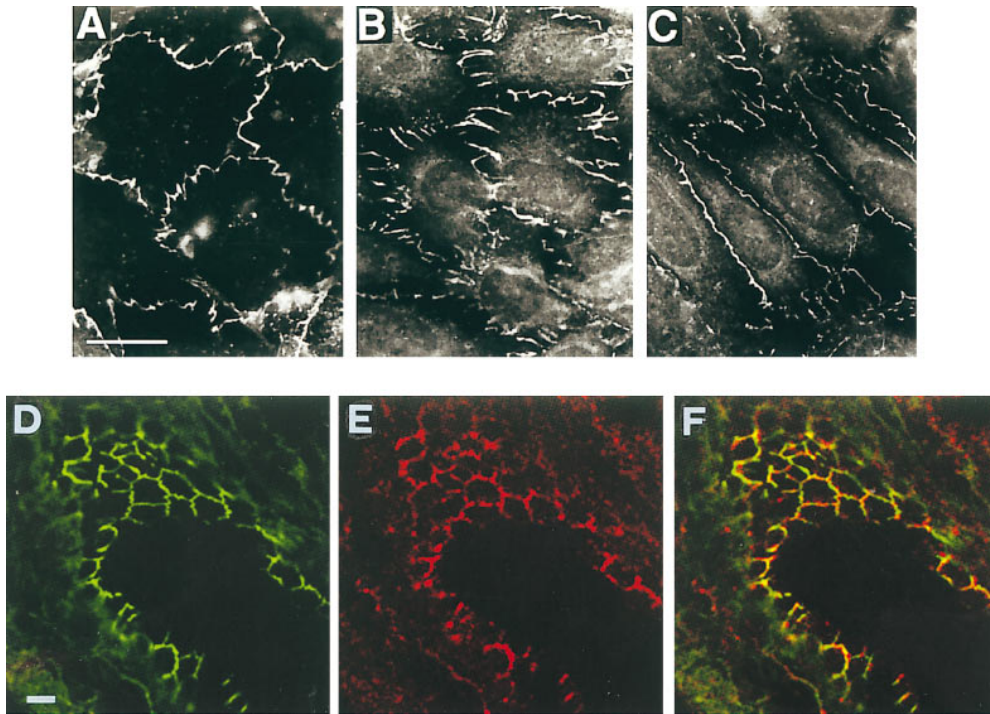
Figure 1. Immunofluorescence analysis of the cellular distribution of BV11 antigen, ZO-1, and VE-cadherin in cultured EC (H5V) monolayers (*A–C*), and of BV11 and cingulin in a section of a small artery of the liver (*D–F*). In cultured EC, BV11 antigen distribution (*A*) shows a cell–cell contact pattern similar to that shown with ZO-1 (*B*) and VE-cadherin (*C*). In artery cryosections, at confocal double-label immunofluorescence microscopy, BV11 antigen (*red fluorescence*; *E*) distributed at cell–cell contacts in a way similar to cingulin (*green fluorescence*; *D*). In merging (*F*), BV11 antigen staining showed colocalization with cingulin in few areas (*yellow fluorescence*; *F*). Bar, 5 μm.

inside the cells, while the antibody recognizes the extracellular domain of JAM. However, the majority of the golden particles are within 25 nm, which is the approximate distance of antigen/immunogold particles.

A summary of the tissue distribution of BV11 is reported in Table I. BV11 antigen was found in EC of different origins. The staining appeared weaker in the high endothelial venules of the lymph nodes (2, 27, 48). BV11 antigen was found in a wide variety of polar epithelia. Interestingly, lens cells, which are rich with AJ but lack TJ, do not bind mAb BV11. BV11 staining was absent in both hematopoietic precursors and mature circulating cells such as leukocytes and erythrocytes, but was positive in megakaryocytes.

Identification and Cloning of BV11 Antigen

A single band of 36–41 kD under reduced conditions was immunoprecipitated from epithelial cells and EC by BV11 mAb (Fig. 4 *A*). The apparent molecular mass was only slightly modified under nonreduced conditions (36–43 kD, not shown).

mAb BV11 was used to screen a cDNA expression library constructed from a murine brain EC line (bEnd.3) as previously described (19, 46, 47, 49). The cDNA library was oligo-dT primed bEnd.3 polyA$^+$ RNA cloned into pCDM8. Three rounds of expression and panning yielded a single clone insert of ~2 kb. The nucleotide and deduced amino acid sequence of this clone is shown in Fig. 5 *A*.

The cDNA insert consists of 2029 nucleotides. The open reading frame gives a predicted polypeptide sequence of 300 amino acids, and has the typical feature observed in a type I integral membrane protein. A potential initiating methionine at nucleotide position 71 is followed by a putative signal peptide that may be cleaved between Leu 23 and Val 24, leaving 215 residues in the extracellular domain of the mature protein. A stretch of 17 hydrophobic residues (Ile 239→Phe 255) presents a potential transmembrane region, and there are 45 residues in the cytoplasmic domain. The extracellular portion contains two domains with intrachain disulfide bonds typical of immunoglobulin-like loops of the V-type (see the schematic representation in Fig. 5 *B*; 8, 29). The difference between the predicted protein of 32 kD and that observed with immunoprecipitation indicated that the *N*-linked glycosylation sites are used by the cells. In fact, when cells were treated with tunicamycin (1 mg/ml overnight), the band immunoprecipitated by BV11 was thinner and shifted to ~29 kD, which corresponds to the predicted molecular mass of the core protein (data not shown). COS cells transfected with the BV11 cDNA synthesized a protein that could be immunoprecipitated by BV11 mAb, and showed a molecular mass comparable to that found in EC. Northern blot analysis of organ extracts showed one species of RNA of ~2 kb (Fig. 4 *B*) in mouse lung, spleen, brain, and heart.

Transfected BV11 Antigen Clusters at Intercellular Junctions and Promotes Cell–Cell Adhesion

When BV11 antigen was transfected in CHO cells as reported in Fig. 6 *B* (10), it concentrated at intercellular junctions in confluent cultures. In sparse cells, the antigen was found only in the areas of cell–cell contacts, and remained diffuse or absent at free cell borders (Fig. 6 *A*). In mixed cultures of BV11 and control transfectants, BV11 antigen did not concentrate at intercellular junctions when transfected cells were in contact with control transfectants (not shown).

To evaluate the ability of BV11 to promote intercellular adhesion, we measured the paracellular permeability of transfectant monolayers using Transwell filters in vitro (10). CHO cells are particularly suitable for this assay
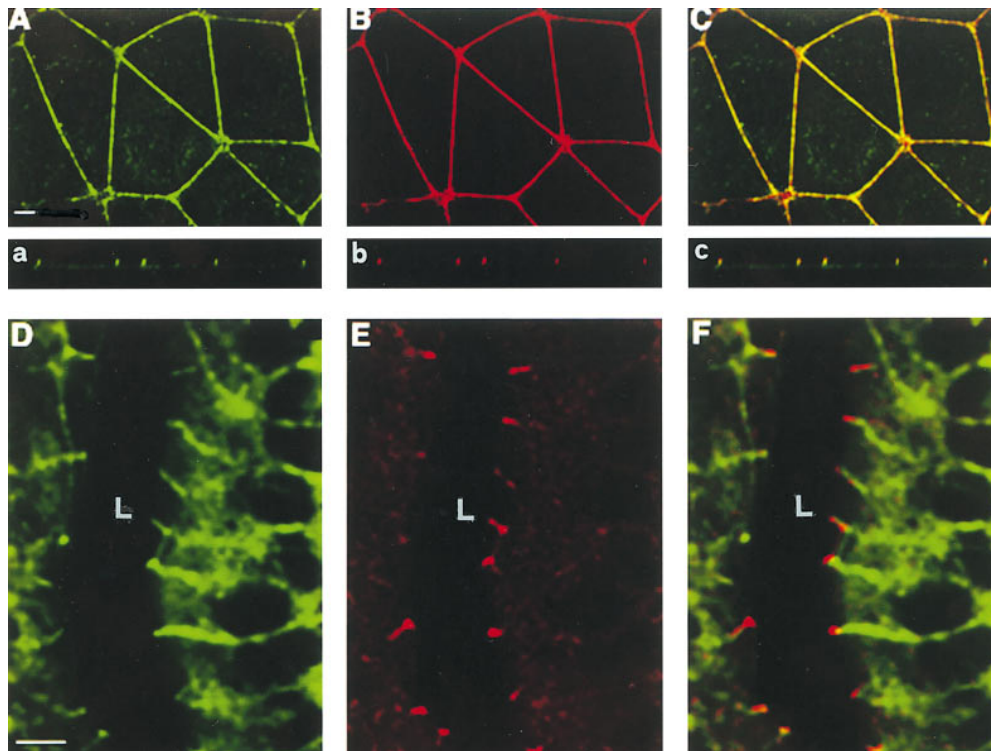
Figure 2. Immunofluorescence analysis of the cellular BV11 antigen distribution in cultured epithelial cells (*A–C, a–c*) and in a tissue section of a mouse duodenum (*D–F*). Cultured epithelial cells (PDV) were costained with cingulin (*green fluorescence; A, a*) and BV11 mAb (*red fluorescence; B, b*). Confocal laser-scanning micrographs of horizontal (*A, B*) and vertical (*a, b*) focal planes, and merging of the two staining patterns (*yellow fluorescence; C and c*) are shown. BV11 and cingulin codistributed at the immediate subapical level of the intercellular cleft. Thickness of cultured epithelial cells is 5–8 μm. Cryosections of the epithelium of the mouse duodenum were costained with β-catenin (*D*) and BV11 mAb (*E*). The merging of the two staining patterns is shown in *F*. BV11 was restricted at the apical region of the cell junctions, and did not colocalize with β-catenin, which was more diffusely distributed along the lateral side of the membrane. L, lumen. Bars, 5 μm.

since untransfected cells do not express cadherins (10) or organized TJ (I. Martìn-Padura, unpublished observations). As shown in Fig. 6 *C*, paracellular permeability was reduced by 50% in BV11 transfectants, and this activity was inhibited in the presence of EGTA. Adding EGTA to control CHO cells did not modify permeability. As a comparison, paracellular permeability was reduced in VE -and *N*-cadherin CHO transfectants in a way comparable to

Figure 3. (*A* and *B*) Electron microscopy localization of BV11 antigen (JAM) on ultrathin cryosections of the epithelium of mouse duodenum. The gold particles decorated the tight junction (*TJ*) area (*arrows*). The immunogold was absent from adherens junction (*zonula adhaerentes, ZA*) and desmosomes (*D*). Bars, 0.1 μM.
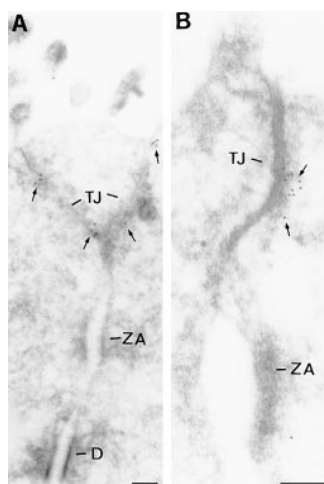
JAM transfectants. In contrast, permeability remained unaffected in transfectants expressing a mutant of VE-cadherin lacking the cytoplasmic domain responsible for catenin binding (39). Truncated VE-cadherin is correctly expressed on CHO cell membrane in amounts comparable to the wild-type form (39). This last result confutes the possibility that reduction in paracellular permeability is an unspecific consequence of CHO transfection with membrane associated proteins.

Overall, these data suggest that BV11 promotes cell–cell adhesion. For this property and for its localization at junctions we propose the name JAM (junctional adhesion molecule) for the BV11 antigen.

Another mAb, BV12, raised against H5V endothelial cells, was found to recognize the same antigen by immunoprecipitation analysis and ELISA on JAM recombinant fragments (see Materials and Methods), H5V, and CHO transfected with JAMcDNA (not shown). As reported in Fig. 7, this mAb, similarly to BV11, decorated cell–cell contacts in endothelial and epithelial cells and in CHO JAM transfectants.

mAb BV11 Inhibits Monocyte Transmigration Through Endothelial Cell Monolayers

The distribution and structural data suggest the possibility that JAM, similarly to PECAM-1, could play a role in leukocyte transmigration. We therefore tested this possibility.

Table I. Distribution of BV11 Antigen (JAM) in Tissue Sections

Cells	Distribution
Endothelial	
Endocardium	++
Arteries	++
Arterioles	++
Veins	++
Venules	+
Capillaries	++
High endothelial venules	+
Brain large vessels	++
Brain capillaries	++
Brain penetrating vessels	++
Choroid plexus vessels	++
Blood	
Hematopoietic precursors	−
Monocytes	−
Granulocytes	−
Erythrocytes	−
Megakaryocytes	++
Epithelial	
Squamous epithelium	++
Skin	++
Oral cavity	++
Esophagus	++
Respiratory epithelium	++
Nasal cavity	++
Trachea	++
Bronchus	++
Intestinal epithelium	++
Renal epithelium	+
Hepatocytes	±
Breast glands	++
Thyroid glands	++
Choroid plexus epithelium	++
Lens epithelium	−
Mesenchymal	
Fibroblasts	−
Mesothelial cells	+

Tissue distribution of BV11 mAb was evaluated using immunohistochemistry on cryostat sections from adult mice organs, newborn mice and 14-d fetuses. For details see Materials and Methods. 600×.

Figure 4. (*A*) Immunoprecipitation analysis of BV11 antigen in different cultured cells. Biotinylated whole-cell extracts were obtained from confluent EC (H5V, lane *1*), epithelial cells (PDV, lane *2*), COS cells transfected with the full length cDNA of mouse JAM (lane *3*), and COS cells transfected with the empty pCDM8 plasmid (lane *4*) and immunoprecipitated as described in Materials and Methods, showing a single band of 36–41 kD under reduced conditions. Migration of molecular weight markers is reported on the left. (*B*) Northern blot analysis of mRNA expression in different murine organs: lung (lane *1*), spleen (lane *2*), brain (lane *3*), and heart (lane *4*). Migration of the molecular mass markers is indicated on the left.

As reported in Fig. 8 *A*, spontaneous monocyte transmigration through EC monolayers was inhibited by the BV11 mAb. This effect was specific since an irrelevant mAb of the same isotype (MK 2.7, IgG2b) able to bind to EC, another mAb directed to JAM (BV12), or an mAb to CD34 (24) that also concentrates at intercellular contacts, had no effect. In addition, F(ab′) fragments of BV11 retained inhibitory activity. Overall, these data confute the possibility that nonspecific or Fc-mediated effects of bound mAb are responsible for the inhibition seen with mAb BV11.

The effect of mAb BV11 was then tested on chemokine-induced monocyte transmigration. MCP-1 and MCP-3 were used as chemoattractants for their specific activity on mononuclear cells (53; Fig. 8 *B*). BV11 was able to reduce monocyte transmigration induced by MCP-1 and MCP-3 by 42% ($P < 0.01$) and by 51% ($P < 0.01$), respectively.

Finally, BV11 was found inhibitory when monocyte chemotaxis was induced by LPS activation of EC (Fig. 8 *C*). After stimulating EC for 24 h with LPS (50 ng/ml), a twofold increase in monocyte transmigration was found.
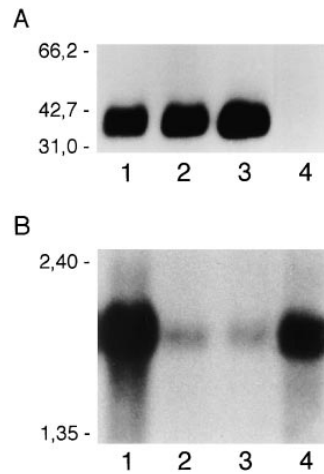
Treatment with BV11, but not with an irrelevant mAb IgG2b, blocked transmigration. LPS treatment of EC did not induce a significant increase in JAM expression as evaluated by FACS analysis and ELISA (data not shown).

Monocyte adhesion to EC measured as number of cells that remained bound to the apical surface of the EC plus transmigrated cells was not modified by BV11 (data not shown). The lack of effect of BV11 on monocyte adhesion was further confirmed by adding Cr^{51}-labeled monocytes to confluent EC in the presence of the antibody, as previously described (1). BV11 up to a concentration of 5 μg/ml did not alter spontaneous monocyte adhesion to EC for up to 60 min of incubation (not shown).

When monocyte chemotaxis to MCP-1 (59) was measured in Transwell chambers in the absence of EC, BV11 was inactive (not shown). This result excludes the possibility that the antibody could unspecifically inhibit monocyte motility and chemotaxis.

mAb BV11 Inhibits Monocyte Infiltration in a Model of Skin Inflammation in Mice

We then moved to an in vivo assay of skin inflammatory reaction in the mouse. The air pouch system was used (18, 44). The treatment scheme is illustrated in Fig. 9 *A*: MCP-3 was injected in the pouch, and the number of emigrated mononuclear cells was then evaluated. MCP-3 caused emigration of $1.57 \pm 0.39 \times 10^6$ cells after 1 h, which is three times the number obtained after saline ($0.49 \pm 0.19 \times 10^6$) or vehicle ($0.58 \pm 0.38 \times 10^6$; carboxymethylcellulose) injection; 70% (± 3%) of the emigrated cells were monocytes. As reported in Fig. 9 *B*, administration of BV11 to mice blocked MCP-3–induced mononuclear cell emigration, while injection of an irrelevant purified mAb of the same isotype had no effect.

Circulating cell counts (monocytes and neutrophils) were monitored 30 min after antibody injection and just before animal death, and showed no significant changes from baseline.

A

```
1                                                                                              G ATC CCT CGA
11    CCT CGA GAT CCA TTG TGC TGG AAA GGT TGC TGT GCC CGT CGC GTC GGG ATT GTA ACT GTA
71    ATG GGC ACC GAG GGG AAA GCC GGG AGG AAA CTG TTG TTT CTC TTC ACG TCT ATG ATC CTG
1      M   G   T   E   G   K   A   G   R   K   L   L   F   L   F   T   S   M   I   L
131   GGC TCT TTG GTA CAA GGC AAG GGT TCG GTG TAC ACT GCT CAA TCT GAC GTC CAG GTT CCC
21     G   S   L   V   Q   G   K   G   S   V   Y   T   A   Q   S   D   V   Q   V   P
191   GAG AAC GAG TCC ATC AAA TTG ACC TGC ACC TAC TCT GGC TTC TCC TCT CCC CGA GTG GAG
41     E   N   E   S   I   K   L   T  [C]  T   Y   S   G   F   S   S   P   R   V   E
251   TGG AAG TTC GTC CAA GGC AGC ACA ACT GCA CTT GTG TGT TAT AAC AGC CAG ATC ACA GCT
61     W   K   F   V   Q   G   S   T   T   A   L   V   C   Y   N   S   Q   I   T   A
311   CCC TAT GCG GAC CGA GTC ACC TTC TCA TCC AGT GGC ATC ACG TTC AGT TCT GTG ACC CGG
81     P   Y   A   D   R   V   T   F   S   S   S   G   I   T   F   S   S   V   T   R
371   AAG GAC AAT GGA GAG TAT ACT TGC ATG GTC TCC GAG GAA GGT GGC CAG AAC TAC GGG GAG
101    K   D   N   G   E   Y   T  [C]  M   V   S   E   E   G   G   Q   N   Y   G   E
431   GTC AGC ATC CAC CTC ACT GTG CTT GTA CCT CCA TCC AAG CCG ACG ATC AGT GTC CCC TCC
121    V   S   I   H   L   T   V   L   V   P   P   S   K   P   T   I   S   V   P   S
491   TCT GTC ACC ATT GGG AAC AGG GCA GTG CTG ACC TGC TCA GAG CAT GAT GAT GGT TCC CCA CCC
141    S   V   T   I   G   N   R   A   V   L   T  [C]  S   E   H   D   G   S   P   P
551   TCT GAA TAT TCC TGG TTC AAG GAC GGG ATA TCC ATG CTT ACA GCA GAT GCC AAG AAA ACC
161    S   E   Y   S   W   F   K   D   G   I   S   M   L   T   A   D   A   K   K   T
611   CGG GCC TTC ATG AAT TCT TCA TTC ACC ATT GAT CCA AAG TCG GGG GAT CTG ATC TTT GAC
181    R   A   F   M   N   S   S   F   T   I   D   P   K   S   G   D   L   I   F   D
671   CCC GTG ACA GCC TTT GAT AGT GGT GAA TAC TAC TGC CAG GCC CAG AAT GGA TAT GGG ACA
201    P   V   T   A   F   D   S   G   E   Y   Y  [C]  Q   A   Q   N   G   Y   G   T
731   GCC ATG AGG TCA GAG GCT GCA CAC ATG GAT GCT GTG GAG CTG AAT GTG GGG GGC ATC GTG
221    A   M   R   S   E   A   A   H   M   D   A   V   E   L   N   V   G   G   I   V
791   GCA GCT GTC CTG GTA ACA CTG ATT CTC CTT GGA CTC TTG ATT TTT GGC GTC TGG TTT GCC
241    A   A   V   L   V   T   L   I   L   L   G   L   L   I   F   G   V   W   F   A
851   TAT AGC CGT GGA TAC TTT GAA ACA ACA AAG AAA GGG ACT GCA CCG GGT AAG AAG GTC ATT
261    Y   S   R   G   Y   F   E   T   T   K   K   G   T   A   P   G   K   K   V   I
911   TAC AGC CAG CCC AGT ACT CGA AGT GAG GGG GAA TTC AAA CAG ACC TCG TCG TTC CTG GTG
281    Y   S   Q   P   S   T   R   S   E   G   E   F   K   Q   T   S   S   F   L   V
971   TGA CCT GCT GCG GCT CCT CCG TTG TCC ATT TGC CTT ACT CAG GTG CTA CAG GTT CCA GCC
301    *
1031  CCT GCT GCT GTA GCT GCA CAG GAT GCC TTC AAT GTC TTC TAG GTC CCA CAG GAC CCC TTG
1091  CTT TTA TTC TAG CTA GGA TAT AAA TTT AAA AAC ATC TAC TTC CCC CTC CTC TTT CCC
1151  ACC CTC CCT CCT TTC CTT ACC ACC ATT GGG TGG CCC GAG ACT AAT TAC AAA GTT TTC GTT
1211  CCC CAT TCC TAT GTG GGA TTG GGC AAG AGT CCT AGA CTA GAC AGT AAT AGT GGC TGG GCT
1271  GAC AGG AAC CCA AAC CAA TAC CTG GCT GTA AAG GCC TCT GAA TAA GGA CTT TAA GCC TAG
1331  CTC CCT GCT TTC TCC TCC CCG GAT GGG GTG CCA GCT ACT CTA GCA GGG GAG CCT GCA GAA
1391  AGG AGG GGC TGA GGA TGG TGA CCT CAG GTC TCT AGT CTT CGG AGC CTC TCT TCT GTC TCC
1451  ACA AAA TGT GCC ACT GGG ATT CTC CTG GAT TCA AAG TAA ACT GAC ATG GTG TCC GTA CGA
1511  GGT GGG AGA GCT CTG TTA GCT CCC AAG AGA CTT GGA GTA AGA AAG ATT TAA AGT GAT CTA
1571  AAG AAA AGG CTG GAA CTG GTG GCC ATT AGT CAC TCT TCA TTT GGC TGG AAC TAC CGC ACG
1631  GAC CCT TTG AAG ATA TGT GTG GAT GGA GAA GAT ACG AGC TTT ATA GTC TGT CTT CTT TGG
1691  TGG CCT CCT GTG TGT GTG TGT GTG TGT GTG TGT GTG TGT GTG TGT GTG AGA GAG AGA GAG
1751  AGA GAG AGA GAG AGA GAG AGA GAG AGA GAG TTG TAA ATT GAT ATT GTT ATA TAG AAG GGG
1811  CTT TCT AGC TCT TTG GCA GGG TTG TGT TTC TGT GTG TTT ATA TTT GAC AGA TGT TGC TGG
1871  AAA TAA AAA CTT CAT TTG ACA GAA AAA AAA AAG CTC TGG CTC CTA GCA CCA TGA AGA TCA
1931  AGA TCA TTG CTC CTC CTG AGC GCA AGT ACT CTG TGT GGA TCG TGT GCT CCA TCC TGG CCT
1991  CAC TGT CCA CCT TCC AGC AGA TGT GGA TCA GCA AGC TT
```

B
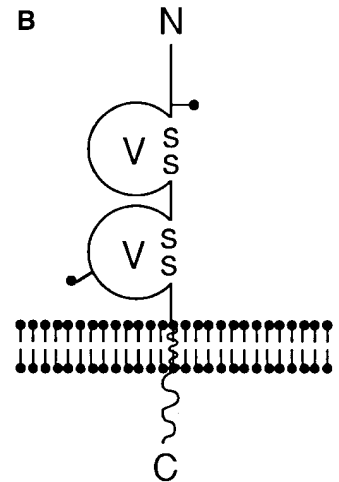
Figure 5. (A) Nucleotide and deduced amino acid sequence of murine BV11 antigen (JAM) cDNA. The putative hydrophobic signal peptide (*dotted underlined*) and transmembrane sequences (*underlined*) are marked. Potential *N*-linked glycosylation sites are marked in bold and underlined at positions 42 and 185. Putative phosphorylation sites are marked in bold. Cysteines likely to form disulfide bonds in the two Ig domains (V-type) are boxed. These sequence data are available from GenBank, European Molecular Biology Laboratory, and DNA Data Base of Japan under the accession code U89915. (B) Structural model for murine JAM. The extracellular portion contains two domains with intrachain disulfide bonds typical of immunoglobulin-like loops of the V-type. Two putative *N*-linked glycosylation sites (—●) are shown.

Discussion

In this study we have identified and cloned a new member of the IgSF that localizes at intercellular junctions in the epithelium and endothelium of different origins. For its type of cellular distribution and its adhesive properties (see below), we propose for this newly described protein the name JAM, junctional adhesion molecule.

At a molecular level, JAM is a type I integral membrane protein and presents, at the extracellular region, two domains with intrachain disulfide bonds typical of Ig loops of the V-type. Searches of available DNA and protein data bases revealed no direct sequence similarities with any known protein with the exception of A33 antigen, which is a recently cloned intestine-specific Ig protein (30). The V-V is a novel arrangement of Ig domains, and JAM is not a member of any subfamily of the IgSF (8).

The distribution of two anti JAM mAbs (BV11 and BV12) in cultured endothelial and epithelial cells shows strict localization at cell–cell contacts. At confocal and immunoelectron microscopy in cell culture and in vivo sections, JAM is found to be concentrated at the apical region of intercellular junctions in correspondence to TJ. In addition, codistribution with TJ markers such as cingulin or occludin can be observed.

JAM cDNA transfection into CHO cells leads to localization of the protein at cell–cell contacts. This localization is apparent only in confluent monolayers and when neighboring cells express JAM. In mixed cultures when JAM transfectants are in contact with control transfectants, the protein remains diffuse, indicating that JAM clustering is due to homotypic interaction.

JAM expression reduces the paracellular permeability of cell monolayers, suggesting that this molecule promotes cell–cell adhesion. In the same experimental system, other molecules known to mediate homophilic adhesion such as VE- or N-cadherin induce a similar reduction in paracellular permeability when transfected in CHO cells. This ef-
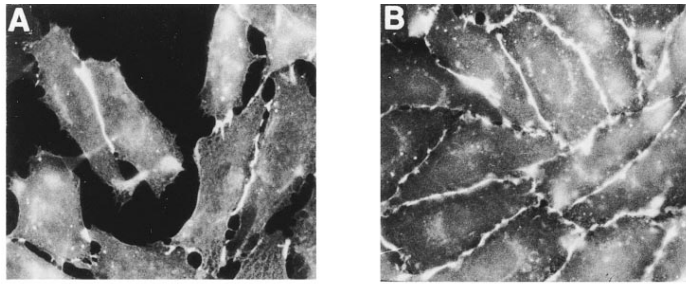
Figure 6. Immunofluorescence analysis of BV11 mAb distribution in CHO cells transfected with JAM, and evaluation of paracellular permeability of transfectant monolayers. In sparse JAM-CHO cells the BV11 staining pattern is restricted to the areas of cell–cell contacts (*A*), while in confluent monolayers BV11 mAb distributed all along the intercellular junctions (*B*). Permeability of control CHO cell monolayers (*pECE-CHO*) to FITC-dextran was reduced by JAM transfection (*JAM-CHO*), and adding EGTA (*JAM-CHO+EGTA*) abolished this difference (*C*). EGTA did not modify permeability of control CHO cells (*pECE-CHO+EGTA*). Transfection of VE-cadherin (*VE-CAD*) and N-cadherin (*N-CAD*) reduced paracellular permeability in a way similar to JAM transfection. In contrast, transfection of truncated VE-cadherin (*tVE-CAD*) was ineffective. Samples from three different wells from three independent experiments were grouped. Overlapping results were obtained when similar experiments were performed with three other independent clones of control and transfectant cells.
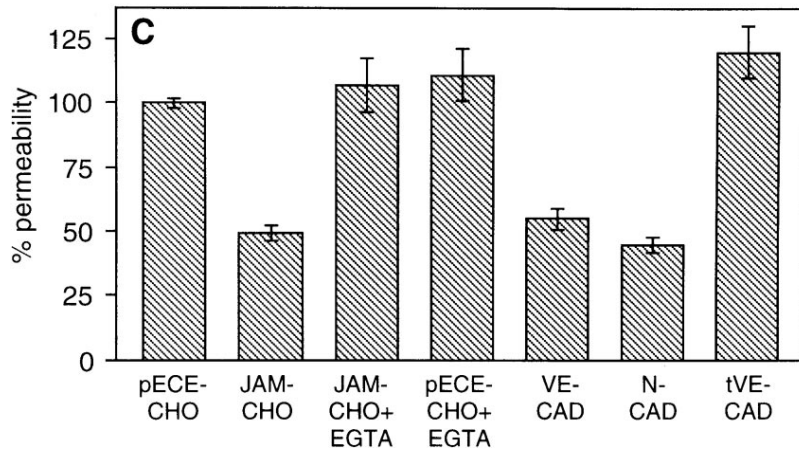
fect seems specific since transfection of a truncated mutant of VE-cadherin that was expressed on the cell membrane with an efficiency comparable to that of the wild-type form (39) was ineffective.

In contrast to these findings, in preliminary experiments JAM-CHO transfectants did not aggregate in suspension

Figure 7. Immunofluorescence analysis of BV12 mAb distribution in CHO cells transfected with JAM (*A*), control CHO cells (*B*), H5V endothelial cells (*C*), and PDV epithelial cells (*D*). Similarly to BV11 (see Figs. 1, 2, and 6), BV12 staining pattern is restricted to the areas of cell–cell contacts in all the cells expressing JAM. Bar, 5 μm.

(not shown). A possible explanation for this discrepancy is that detachment of the cells could alter JAM conformation and/or cause a slight digestion of biologically active epitopes so that the molecule loses its adhesive properties. Interestingly, VE-cadherin presents a similar behavior since it is poorly active in promoting homotypic aggregation of cells in suspension, but significantly reduces paracellular permeability (10). For VE-cadherin, the effect on permeability requires its anchorage to catenins and the actin cytoskeleton since a truncated mutant of the molecule is ineffective (39 and the present paper). We still do not know whether JAM is linked to the cell cytoskeleton or whether this association is required for its adhesive activity. If this requirement for JAM association to the cytoskeleton is the case, it is possible that when cells are in suspension and the organization of the cytoskeleton is modified, JAM activity is inhibited.

The distribution of JAM at TJ tempts us to speculate that this protein participates in the assembly and organization of these structures, and directly interacts with TJ components. However, further studies are required to prove this possibility directly.

When compared with occludin, JAM presents a different biological behavior. It has been reported that transfected occludin concentrates at intercellular junctions and confers adhesion mostly in cells that already express organized AJ or TJ (6, 54). JAM seems to act independently from preorganized junctional structures. The CHO cells used in this work do not express cadherins (10), and do not present organized TJ at electron microscopy (I. Martìn-Padura, unpublished results). However, when transfected with JAM, the cells are able to concentrate this protein at intercellular contacts. This behavior is similar to that of other junctional proteins such as PECAM or VE-cadherin.
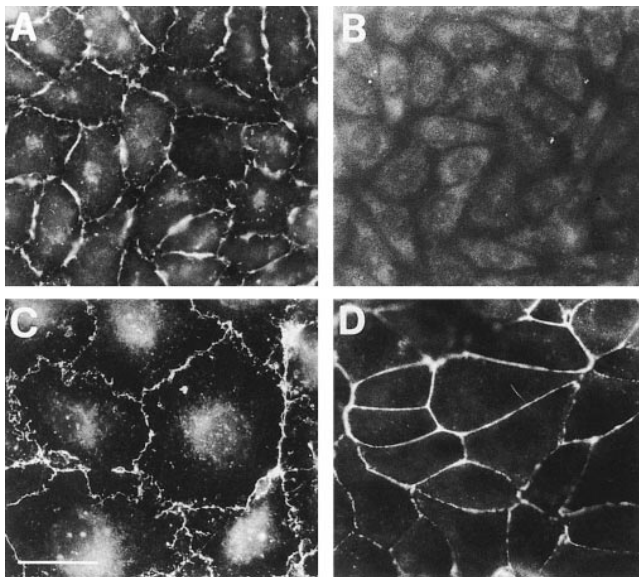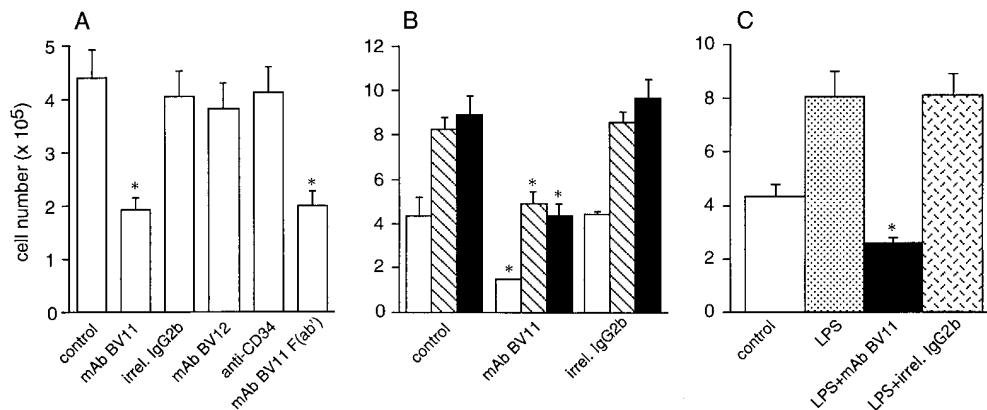
Figure 8. Effect of JAM antibodies on transendothelial migration of monocytes in vitro. (*A*) Spontaneous monocyte migration across EC monolayers in vitro is inhibited by mAb BV11 (IgG and F(ab') fragments), but not by anti-JAM mAb BV12 nor anti-CD34 (MEC 14) mAb. An irrelevant mAb (MK 2.7) of the same isotype (IgG2b) of BV11 was also inactive. (*B*) Anti-JAM mAb BV11 blocks spontaneous (*open bars*), MCP-1 (100 ng/ml; *hatched bars*), and MCP-3 (100 ng/ml)–induced migration (*solid bars*) of monocytes across EC monolayers in vitro. (*C*) mAb BV11 inhibited monocyte transmigration through LPS-treated EC monolayers. EC were incubated with LPS (50 ng/ml) for 24 h, and were then washed before monocyte addition as described. Data are mean of at least three experiments performed in quadruplicates. Error bars, SD. *$P < 0.001$ by analysis of variance and Dunnett's test in comparison to values obtained in absence of antibodies.
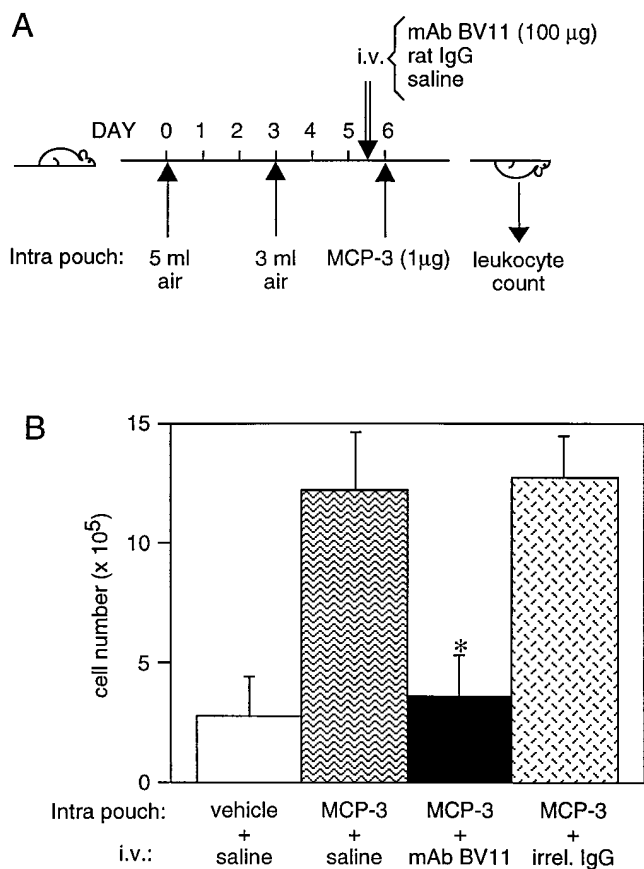
Figure 9. (*A*) Treatment scheme of the air pouch model of skin inflammation in mice. Two different volumes of air were injected subcutaneously in the animals at 3-d intervals. BV11 or an irrelevant purified mAb (HB151) of the same isotype or saline were administered intravenously (i.v.) 60 h after the second air injection. 12 h later MCP-3 was injected intrapouch. After 1 h mice were killed, and the pouches were washed with 1 ml of saline. Mononuclear cells present were stained with erythrosin and counted. (*B*) Effect of BV11 mAb on MCP-3–induced monocyte

It is possible that JAM participates in the first steps of intercellular contact formation through homophilic clustering, and that only a second time gets incorporated in TJ.

A major finding of the present study is that a JAM mAb, BV11, was able to inhibit monocyte transmigration through endothelial monolayers in vitro and to block monocyte infiltration in a skin inflammatory model in vivo.

This effect was not mediated by unspecific Fc receptor binding since F(ab') fragments of the mAb retain the activity, and since another mAb of the same isotype able to bind EC was inactive. In addition, the effect was specific for BV11 since another available mAb directed to JAM (BV12), but recognizing a different epitope (see Materials and Methods), was ineffective.

BV11 inhibited not only spontaneous monocyte transmigration but also transmigration induced by adding monocyte-specific chemokines (MCP-1 or MCP-3) or by activating the endothelial cell monolayers with LPS. This result suggests that BV11 exerts a specific and general effect on transmigration. Indeed, BV11 does not influence monocyte chemotaxis through empty filters, and does not change monocyte adhesion to endothelial cells, indicating that its activity is not due to inhibition of monocyte reactivity to chemokines or to adhesion molecules.

The data obtained in vitro using chemotaxis assays were confirmed in an in vivo model of skin inflammation. In this model the mAb BV11 was strongly effective, and essentially blocked monocyte transmigration to MCP-3. The effect of the mAb seems specific since the same dose of an irrelevant mAb of the same isotype was ineffective.

emigration in the air pouch model in vivo. The figure reports the results of typical experiments out of at least three performed. Error bars, SD. *$P < 0.001$ by analysis of variance and Dunnett's test in comparison to values obtained in the absence of antibodies.

In addition, mice deficient of the complement component C1q (58) were equally responsive to mAb BV11 (M. Romano and P. Fruscella, unpublished data), excluding in this way a role of complement activation in the observed inhibition.

The mechanism of action of mAb BV11 and of JAM in general is still unknown. A possibility is that JAM, for its localization at intercellular contacts, binds monocytes and directs their migration through the intercellular cleft. Other proteins such as the matrix protein hevin have been suggested to modulate transendothelial migration of lymphocytes by facilitating their motility (27). A similar mechanism has also been hypothesized for another junctional immunoglobin such as PECAM-1, which is located in a less apical domain of the interendothelial cleft (5). PECAM is unable to induce leukocyte adhesion, but appears to be required for their extravasation (38). It is possible that these two proteins collaborate in promoting cell movement through the interendothelial junctions by acting at different regions of the intercellular cleft.

An important question is related to JAM counterreceptor on monocytes. mAb BV11 does not recognize monocytes, and does not change endothelial cell or JAM-CHO transfectant paracellular permeability, strongly suggesting that this mAb does not exert its activity by inhibiting homotypic binding. It is conceivable that monocytes recognize this protein through a heterotypic type of interaction inhibited by mAb BV11. Other immunoglobulins, including PECAM, have been found to express both homophilic and heterophilic types of interactions (32).

In conclusion, in this paper we report the identification and cloning of a new member of the immunoglobulin family with a so far undescribed V-V structure that we called JAM. This protein concentrates at endothelial and epithelial junctions, and codistributes with TJ components. The mAb BV11 directed to JAM inhibits monocyte transmigration in vitro and in vivo, strongly suggesting that this molecule is relevant in the control of monocyte infiltration in inflammatory conditions.

The mechanism of action of JAM requires further investigation, but the data reported strongly support the concept that manipulation of the molecular organization of endothelial junctions could be an effective approach in controlling endothelial permeability and monocyte traffic.

References

1. Allavena, P., C. Paganin, I. Martin-Padura, G. Peri, M. Gaboli, E. Dejana, P.C. Marchisio, and A. Mantovani. 1991. Molecules and structures involved in the adhesion of natural killer cells to vascular entothelium. *J. Exp. Med.* 173:439–448.
2. Anderson, A.O., and S. Shaw. 1993. T cell adhesion to endothelium: the FRC conduit system and other anatomic and molecular features which facilitate the adhesion cascade in lymph node. *Semin. Immunol.* 5:271–282.
3. Anderson, J.M., M.S. Balda, and A.S. Fanning. 1993. The structure and regulation of tight junctions. *Curr. Opin. Cell Biol.* 5:772–776.
4. Anderson, J.M. and C.M. Van Itallie. 1995. Tight junctions and the molecular basis for regulation of paracellular permeability. *Am. J. Physiol.* 269: G465–G475.
5. Ayalon, O., H. Sabanai, M.-G. Lampugnani, E. Dejana, and B. Geiger. 1994. Spatial and temporal relationships between cadherins and PECAM-1 in cell-cell junctions of human endothelial cells. *J. Cell Biol.* 126: 247–258.
6. Balda, M.S., J.A. Whitney, C. Flores, S. Gonzalez, M. Cereijido, and K. Matter. 1996. Functional dissociation of paracellular permeability and transepithelial electrical resistance and disruption of the apical-basolateral intramembrane diffusion barrier by expression of a mutant tight junction membrane protein. *J. Cell Biol.* 134:1031–1049.
7. Bogen, S., J. Pak, M. Garifallou, X. Deng, and W.A. Muller. 1994. Monoclonal antibody to murine PECAM-1 (CD31) blocks acute inflammation in vivo. *J. Exp. Med.* 179:1059–1064.
8. Bork, P., L. Holm, and C. Sander. 1994. The immunoglobulin fold: structural classification, sequence patterns and common core. *J. Mol. Biol.* 242:309–320.
9. Breier, G., F. Breviario, L. Caveda, R. Berthier, U. Schnurch, D. Gotsch, D. Vestweber, W. Risau, and E. Dejana. 1996. Molecular cloning and expression of murine vascular endothelial-cadherin in early stage development of cardiovascular system. *Blood.* 87:630–642.
10. Breviario, F., L. Caveda, M. Corada, I. Martin-Padura, P. Navarro, J. Golay, M. Introna, D. Gulino, M.G. Lampugnani, and E. Dejana. 1995. Functional properties of human vascular endothelial cadherin (7B4/cadherin-5) an endothelial specific cadherin. *Arterioscler. Thromb. Vasc. Biol.* 15:1229–1239.
11. Citi, S. 1993. The molecular organization of tight junctions. *J. Cell Biol.* 121: 485–489.
12. Citi, S., H. Sabanay, R. Jakes, B. Geiger, and J. Kendrick-Jones. 1988. Cingulin, a new peripheral component of tight junctions. *Nature.* 333:272–276.
13. Citi, S., H. Sabanay, J. Kendrick-Jones, and B. Geiger. 1989. Cingulin: characterization and localization. *J. Cell Sci.* 93:107–122.
14. Colotta, F., G. Peri, A. Villa, and A. Mantovani. 1984. Rapid killing of actinomycin D-treated tumor cells by human mononuclear cells.I. Effectors belong to the monocyte-macrophage lineage. *J. Immunol.* 132:936–942.
15. Dejana, E. 1997. Endothelial adherens junctions: implications in the control of vascular permeability and angiogenesis. *J. Clin. Invest.* 98:1949–1953.
16. Dejana, E., M. Corada, and M.-G. Lampugnani. 1995. Endothelial cell-to-cell junctions. *FASEB J.* 9:910–918.
17. Dong, Q.G., S. Bernasconi, S. Lostaglio, R. Wainstok de Calmanovic, I. Martin-Padura, F. Breviario, A. Mantovani, and A. Vecchi. 1997. A general strategy for isolation of endothelial cells from murine tissues: characterization of two endothelial cell lines obtained from murine lung and subcutaneous sponge implants. *Arterioscler. Thromb. Vasc. Biol.* 17: 1599–1904.
18. Edwards, J.C., A.D. Sedgwick, and D.A. Willoughby. 1981. The formation of a structure with features of synovial lining by subcutaneous injection of air: an in vivo tissue culture system. *J. Pathol.* 134:147–156.
19. Fawcett, J., C.L. Holness, L.A. Needham, H. Turley, K.C. Gatter, D.Y. Mason, and D.L. Simmons. 1992. Molecular cloning of ICAM-3, a third ligand for LFA-1, constitutively expressed on resting leukocytes. *Nature.* 360:481–484.
20. Fawcett, J., C. Buckley, C.L. Holness, I.N. Bird, J.H. Spragg, J. Saunders, A. Harris, and D.L. Simmons.1995. Mapping and homotypic binding sites in CD31 and the role of CD31 adhesion in the formation of interendothelial cell contacts. *J.Cell Biol.* 128: 1229–1241.
21. Furuse, M., T. Hirase, M. Itoh, A. Nagafuchi, S. Yonemura, and S. Tsukita. 1993. Occludin: a novel integral membrane protein localizing at tight junctions. *J. Cell Biol.* 123:1777–1788.
22. Furuse, M., M. Itoh, T. Hirase, A. Nagasuchi, S. Yonemura, and S. Tsukita. 1994. Direct association of occludin with ZO-1 and its possible involvement in the localization of occludin at tight junction. *J. Cell Biol.* 127: 1617–1626.
23. Fusening, N.E., D. Breitkreutz, R.T. Dzrlieva, P. Boukamp, E. Hezmann, A. Bohnert, J. Pohlmann, C. Rausch, S. Schutz, and J. Hornung. 1982. Epidermal cell differentiation and malignant transformation in culture. *Cancer Forum.* 6:209–240.
24. Garlanda, C., R. Berthier, J. Garin, A. Stoppacciaro, D. Vittet, D. Goulino, C. Matteucci, A. Mantovani, A. Vecchi, and E. Dejana. 1997. Characterization of MEC 14, a new monoclonal antibody recognizing mouse CD34: a useful reagent for identification and characterization of blood vessels and hematopoietic precursors. *Eur. J. Cell Biol.* 73:368–377.
25. Garlanda, C., C. Parravicini, M. Sironi, M. De Rossi, R. Wainstok de Calmanovici, F. Carozzi, F. Bussolino, F. Colotta, A. Mantovani, and A. Vecchi. 1994. Progressive growth in immunodeficient mice and host cell recruitment by mouse endothelial cells transformed by polyoma middle T: implications for the pathogenesis of opportunistic vascular tumors. *Proc. Natl. Acad. Sci. USA.* 91:7291–7295.

26. Geiger, B., and O. Ayalon. 1992. Cadherins. *Ann. Rev. Cell Biol.* 8:307–332.

27. Girard, J.-P., and T.A. Springer. 1995. High endothelial venules (HEVs): specialized endothelium for lymphocyte migration. *Immunol. Today.* 16: 449–457.

28. Gumbiner, B.M. 1996. Cell adhesion: the molecular basis of tissue architecture and morphogenesis. *Cell.* 84:345–357.

29. Harpaz, Y., and C. Chothia. 1994. Many of the immunoglobulins superfamily domains in cell adhesion molecules and surface receptors belong to a new structural set which is close to that containing variable domains. *J. Mol. Biol.* 238:528–539.

30. Heath, J.K., S.J. White, C.N. Johnstone, B. Catimel, R.J. Simpson, R.L. Moritz, G.-F. Tu, H. Ji, R.H. Whitehead, L.C. Groenen, et al. 1997. The human A33 antigen is a transmembrane glycoprotein and a novel member of the immunoglobulin superfamily. *Proc. Natl. Acad. Sci. USA.* 94: 469–474.

31. Hulksen, J., J. Berhens, and W. Birchmeier. 1994. Tumor-suppressor gene products in cell contacts: the cadherin-APC-armadillo connection. *Curr. Opin. Cell Biol.* 6:711–716.

32. Imhof, B., and D. Dunon. 1995. Leukocyte migration and adhesion. *Adv. Immunol.* 58:345–416.

33. Kemler, R. 1993. From cadherins to catenins: cytoplasmic protein interactions and regulation of cell adhesion. *Trends Genet.* 9:317–321.

34. Keon, B.H., S.S. Schafer, C. Kuhn, C. Grund, and W.W. Franke. 1996. Symplekin, a novel type of tight junction plaque protein. *J. Cell Biol.* 134: 1003–1018.

35. Klymkowsky, M.W., and B. Parr. 1995. The body language of the cells: the intimate connection between cell adhesion and behavior. *Cell.* 83:5–8.

36. Lampugnani, M.G., M. Resnati, M. Raiteri, R. Pigott, A. Pisacane, G. Houen, and L. Ruco. 1992. A novel endothelial-specific membrane protein is a marker of cell-cell contacts. *J. Cell Biol.* 118:1511–1522.

37. Martin-Padura, I., G. Bazzoni, A. Zanetti, S. Bernasconi, M.J. Elices, A. Mantovani, and E. Dejana. 1994. A novel mechanism of colon carcinoma cell adhesion to the endothelium triggered by β1 integrin chain. *J. Biol. Chem.* 269:6124–6132.

38. Muller, W.A., S.A. Weigl, X. Deng, and D.M. Phillips. 1993. PECAM-1 is required for transendothelial migration of leukocytes. *J. Exp. Med.* 178: 449–460.

39. Navarro, P., L. Caveda, F. Breviario, I. Mandoteanu, M.G. Lampugnani, and E. Dejana. 1995. Catenin-dependent and -independent functions of vascular endothelial cadherin. *J. Biol. Chem.* 270:30965–30972.

40. Navarro, P., L. Ruco, and E. Dejana. 1998. Differential localization of VE- and *N*-cadherin in human endothelial cells. VE-cadherin competes with *N*-cadherin for junctional localization. *J. Cell Biol.* 140:1475–1484.

41. Parham, P. 1985. *In* Hanbook of Experimental Immunology in Four Volumes: Immunochemistry. Vol. 14. D.M. Weir, editor. Blackwell Scientific Publications, Oxford. 1–23.

42. Perego, C., A. Bulbarelli, R. Longhi, M. Caimi, A. Villa, M.J. Caplan, and G. Pietrini. 1997. Sorting of two polytopic proteins, the gamma-aminobutyric acid and betaine transporters, in polarized epithelial cells. *J. Biol. Chem.* 272:6584–6592.

43. Rival, Y., A. Del Maschio, M.-J. Rabiet, E. Dejana, and A. Duperray. 1996. Inhibition of platelet endothelial cell adhesion molecule-1 synthesis and leukocyte transmigration in endothelial cells by the combined action of TNF-α and IFN-γ. *J. Immunol.* 157:1233–1241.

44. Romano, M., R. Faggioni, M. Sironi, S. Sacco, B. Echtenacher, E. Di Santo, M. Salmona, and P. Ghezzi. 1997. Carrageenan-induced acute inflammation in the mouse air pouch synovial model. Role of tumor necrosis factor. *Mediat. Inflamm.* 6:1–7.

45. Rubin, L.L. 1992. Endothelial cells: adhesion and tight junctions. *Curr. Opin. Cell Biol.* 4:830–833.

46. Seed, B. 1987. An LFA-3 cDNA encodes a phospholipid-linked membrane protein homologous to its receptor CD2. *Nature.* 329:840–842.

47. Seed, B., and A. Aruffo. 1987. Molecular cloning of the CD2 antigen, the T-cell erythrocyte receptor, by a rapid immunoselection procedure. *Proc. Natl. Acad. Sci. USA.* 84:3365–3369.

48. Simionescu, N., and N.Z. Simionescu. 1991. Endothelial transport macromolecule: transcytosis and endocytosis. *Cell Biol. Rev.* 25:5–80.

49. Simmons, D., M.W. Makgoba, and B. Seed. 1988. ICAM, an adhesion ligand of LFA-1, is homologous to the neural cell adhesion molecule NCAM. *Nature.* 331:624–627.

50. Springer, T.A. 1994. Traffic signals for lymphocyte recirculation and leukocyte emigration: the multistep paradigm. *Cell.* 76:301–314.

51. Stevenson, B.R., J.D. Siciliano, M.S. Mooseker, and D.A. Goodenough. 1986. Identification of ZO-1: a high molecular weight polypeptide associated with the tight junction (*zonula occludens*) in a variety of epithelia. *J. Cell Biol.* 103:755–766.

52. Takeichi, M. 1993. Cadherin in cancer: implications for invasion and metastasis. *Curr. Opin. Cell Biol.* 5:806–811.

53. Van Damme, J., P. Proost, J.P. Lanaerst, and G. Opdenakker. 1997. Structural and functional identification of two human, tumor-derived monocyte chemotactic proteins (MCP-2 and MCP-3) belonging to the chemokine family. *J. Exp. Med.* 176:59–65.

54. Van Itallie, C.M., and J.M. Anderson. 1997. Occludin confers adhesiveness when expressed in fibroblasts. *J. Cell Sci.* 110:1113–1121.

55. Vaporciyan, A.A., H.M. DeLisser, H.-C. Yan, I.I. Mendiguren, S.R. Thom, M.L. Jones, P.A. Ward, and S.M. Albelda. 1993. Involvement of platelet-endothelial cell adhesion molecule-1 in neutrophil recruitment in vivo. *Science.* 262:1580–1582.

56. Vecchi, A., C. Garlanda, M.-G. Lampugnani, M. Resnati, C. Matteucci, A. Stoppacciaro, H. Schnurch, W. Risau, L. Ruco, A. Mantovani, and E. Dejana. 1994. Monoclonal antibodies specific for endothelial cells of mouse blood vessels. Their application in the identification of adult and embryonic endothelium. *Eur. J. Cell Biol.* 63:247–254.

57. Villa, A., P. Podini, M.C. Panzeri, H.D. Soling, P. Volpe, and J. Meldolesi. 1993. The endoplasmic-sarcoplasmic reticulum of smooth muscle: immunocytochemistry of vas deferens fibers reveals specialized subcompartments differently equipped for the control of Ca++ homeostasis. *J. Cell Biol.* 121:1041–1051.

58. Walport, M.J., K.A. Davies, B.J. Morley, and M. Botto. 1997. Complement deficiency and autoimmunity. *Ann. NY Acad. Sci.* 815:267–281.

59. Wang, J.M., A. Sica, G. Peri, S. Walter, I.M. Padura, P. Libby, M. Ceska, I. Lindley, F. Colotta, and A. Mantovani. 1991. Expression of monocyte chemotactic protein and interleukin-8 by cytokine-activated human vascular smooth muscle cells. *Arterioscler. Thromb.* 11:1166–1174.

60. Zocchi, M.R., E. Ferrero, B.E. Leone, P. Rovere, E. Bianchi, E. Toninelli, and R. Pardi. 1996. CD 31/PECAM-1 driven chemokine-independent transmigration of human T lymphocytes. *Eur. J. Immunol.* 26:759–767.